Development of a Fully-Tabulated, Anisotropic and Asymmetric Material Model for LS-DYNA (*MAT_264)

Sean Haight [1], Cing-Dao "Steve" Kan [1], Paul Du Bois [2]

[1] George Mason University – Center for Collision Safety and Analysis (CCSA)
[2] Consulting Engineer, Northville, MI

1 Introduction

The purpose of this research is to develop a fully-tabulated, anisotropic, asymmetric and rate dependent material model for solid elements. Physical tests of several metallic materials have shown to have anisotropic (or orthotropic) characteristics. While many material models in LS-DYNA currently have anisotropic modeling options, they are typically focused on the material forming applications – not crash and impact analysis. Unlike most anisotropic forming material models, this model will have: rate dependency, temperature dependency, tabulated hardening (as opposed to parameterized inputs), associated flow, directional tensile compressive asymmetry and the ability to maintain stability for large deformations.

2 Development

This anisotropic model is an extension of the currently existing Generalized Yield Surface (***MAT_224_GYS**) implementation of the Tabulated Johnson Cook material model (***MAT_224**) [1]. In other words, this model builds upon the currently available features of ***MAT_224** and ***MAT_224_GYS**. Strain rate and temperature dependencies are utilized as independent tabulated values. Hardening curves for tension, compression and shear are also tabulated and independent. Isotropic failure is retained from ***MAT_224** as a function of triaxiality, Lode parameter, strain rate, temperature and element size. Lastly, tabulated hardening for tension and compression will allow the user to specify tensile and compressive yield stress in the 0-degree, 45-degree, 90-degree, and thickness directions (as a function of strain rate).

The first phase of this development was to generalize the ***MAT_224_GYS** yield function (*von Mises*) to a *Hill* yield function [2]. This allows for tabulated inputs for the 0-deg, 45-deg, 90-deg, and thickness directions in tension.

***MAT_224_GYS:** $\sigma_{vm}\left[c_1+c_2\theta_L+c_3\theta_L^2\right]\le\sigma_t\left(\varepsilon_p,\dot{\varepsilon}_p,T\right)$

***MAT_264:** $\sigma_{hill}\left[c_1+c_2\theta_L+c_3\theta_L^2\right]\le\sigma_t\left(\varepsilon_p,\dot{\varepsilon}_p,T\right)$

where: $\sigma_{hill}{}^2 = F(\sigma_{yy}-\sigma_{zz})^2+G(\sigma_{zz}-\sigma_{xx})^2+H(\sigma_{xx}-\sigma_{yy})^2+\ldots$
$L\sigma_{yz}{}^2+L\sigma_{zy}{}^2+M\sigma_{zx}{}^2+M\sigma_{xz}{}^2+N\sigma_{xy}{}^2+N\sigma_{yx}{}^2$

and: $c_1\left(\varepsilon_p,\dot{\varepsilon}_p,T\right)$, $c_2\left(\varepsilon_p,\dot{\varepsilon}_p,T\right)$, $c_3\left(\varepsilon_p,\dot{\varepsilon}_p,T\right)$

The second development phase was to generalize the Lode parameter so that 0-deg, 45-deg 90-deg, and thickness compression can also be input by the user. [3][4][5][6]

***MAT_264:** $\sigma_{hill}\left[c_1+c_2\theta_{L1}+c_3\theta_{L2}^2\right]\le\sigma_{00-t}\left(\varepsilon_p,\dot{\varepsilon}_p,T\right)$

where: $\theta_{L1}=\dfrac{27J_{31}^0}{2\sigma_{vm}^3}$

$$J_{31}^{o} = \frac{1}{27}(b_1 + b_2)\sigma_{xx}^3 + \frac{1}{27}(b_3 + b_4)\sigma_{yy}^3 + \frac{1}{27}(2b_1 + 2b_4 - b_2 - b_3)\sigma_{zz}^3 - \frac{1}{9}(b_1\sigma_{yy} + b_2\sigma_{zz})\sigma_{xx}^2 - \ldots$$
$$\frac{1}{9}(b_3\sigma_{zz} + b_4\sigma_{xx})\sigma_{yy}^2 - \frac{1}{9}((b_1 - b_2 + b_4)\sigma_{xx} + (b_1 - b_3 + b_4)\sigma_{yy})\sigma_{zz}^2 + \frac{2}{9}(b_1 + b_4)\sigma_{xx}\sigma_{zz}\sigma_{yy} - \ldots$$
$$\frac{\sigma_{xz}^2}{3}(2b_9\sigma_{yy} - b_8\sigma_{zz} - (2b_9 - b_8)\sigma_{xx}) - \frac{\sigma_{xy}^2}{3}(2b_{10}\sigma_{zz} - b_5\sigma_{yy} - (2b_{10} - b_5)\sigma_{xx}) - \ldots$$
$$\frac{\sigma_{yz}^2}{3}(-b_7\sigma_{zz} - b_6\sigma_{yy} + (b_6 + b_7)\sigma_{xx}) + 2b_{11}\sigma_{xy}\sigma_{yz}\sigma_{zx}$$

and $\theta_{L2} = \frac{27J_{32}^0}{2\sigma_{vm}^3}$

$$J_{32}^{o} = \frac{1}{27}(d_1 + d_2)\sigma_{xx}^3 + \frac{1}{27}(d_3 + d_4)\sigma_{yy}^3 + \frac{1}{27}(2d_1 + 2d_4 - d_2 - d_3)\sigma_{zz}^3 - \frac{1}{9}(d_1\sigma_{yy} + d_2\sigma_{zz})\sigma_{xx}^2 - \ldots$$
$$\frac{1}{9}(d_3\sigma_{zz} + d_4\sigma_{xx})\sigma_{yy}^2 - \frac{1}{9}((d_1 - d_2 + d_4)\sigma_{xx} + (d_1 - d_3 + d_4)\sigma_{yy})\sigma_{zz}^2 + \frac{2}{9}(d_1 + d_4)\sigma_{xx}\sigma_{zz}\sigma_{yy} - \ldots$$
$$\frac{\sigma_{xz}^2}{3}(2d_9\sigma_{yy} - d_8\sigma_{zz} - (2d_9 - d_8)\sigma_{xx}) - \frac{\sigma_{xy}^2}{3}(2d_{10}\sigma_{zz} - d_5\sigma_{yy} - (2d_{10} - d_5)\sigma_{xx}) - \ldots$$
$$\frac{\sigma_{yz}^2}{3}(-d_7\sigma_{zz} - d_6\sigma_{yy} + (d_6 + d_7)\sigma_{xx}) + 2d_{11}\sigma_{xy}\sigma_{yz}\sigma_{zx}$$

This formulation of the Lode parameter provides 22 independent coefficeients that are used to implement directional asymmetry in the plasticity model. These coefficents are then calculated internally from the provided tabulated hardening curves. In turn, the yield surface size and shape can change with each simulation time step.

3 Verification

3.1 Single element verification (tension)

The first verification simulations were intended to confirm that an isotropic implementation of ***MAT_264** would produce the same results as ***MAT_224_GYS**. To accomplish this, a set of single solid element simulations was designed so that the results of the two models can be directly compared. The simulation design is shown in Figure 1. The first row (from the bottom) is the anisotropic implementation of ***MAT_264**, where different values of yield stress were provided to each element. The second row is an isotropic implementation of ***MAT_264** (where all the yield stresses are identical), and the last row of elements use the isotropic ***MAT_224_GYS** model. The first column (from left to right) is elements taken from the material rolling direction. The second column is material taken from the 45-degree direction (relative to the rolling direction). The last two rows are the 90-degree and thickness directions (relative to the rolling direction).

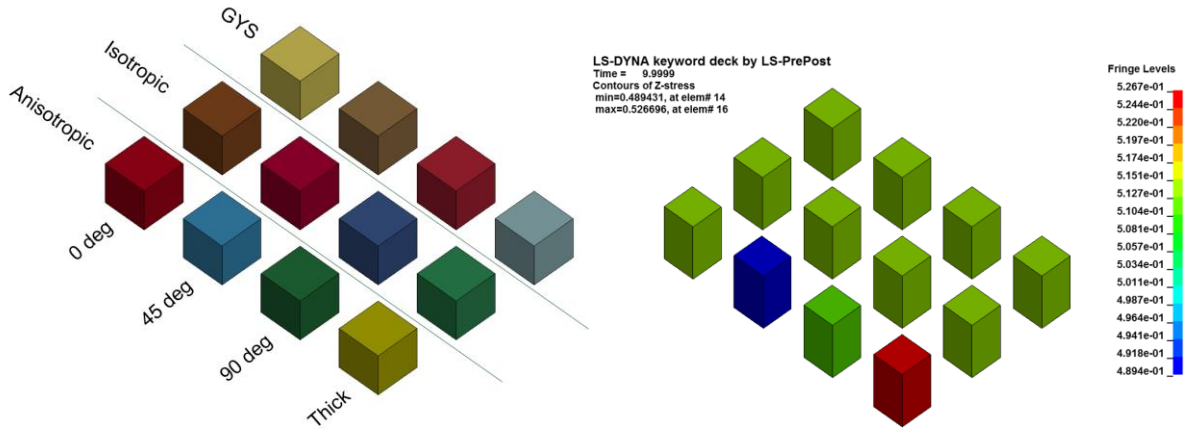

Fig.1: Single element verification simulation (tension) setup (left) and stress results (right)

As shown in Figure 1, the isotropic implementation of ***MAT_264** (row 2) is equivalent to the ***MAT_224_GYS** material model (row 3). Additionally, the anisotropic implementation (with 4 individual tabulated hardening curves) provide different stress levels for each element.

3.2 Single element verification (compression)

The second verification simulation was to confirm that the material model can provide anisotropic results in both tension and compression using a single material model. To accomplish this, a second single element simulation setup was designed. In this simulation, the first row of elements (from the bottom) are deformed in uniaxial tension. The second row of elements are deformed in uniaxial compression. Similar to the first single element simulation, the first column (from the left) of elements is material in the rolling direction, followed by the 45-degree, 90-degree and thickness directions. This simulation setup can be seen in Figure 2.

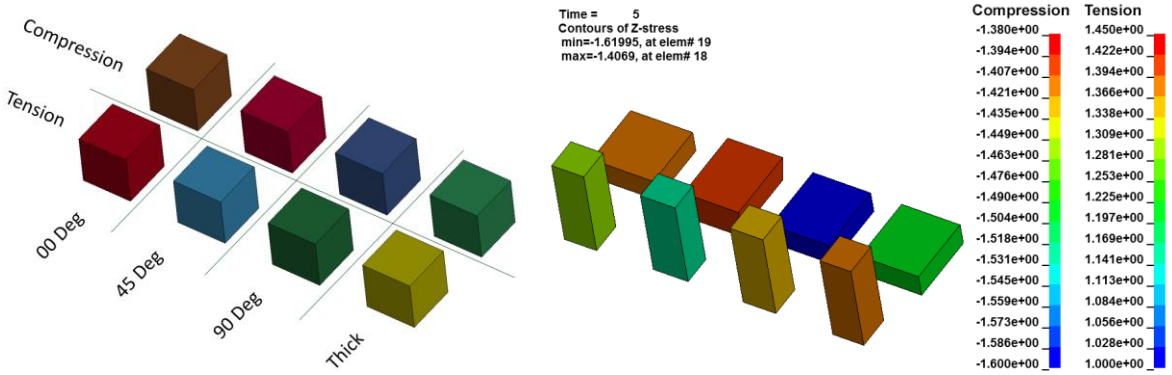

Fig.2: Single element verification simulation (tension and compression) setup (left) and stress results (right)

As shown in Figure 2, each element exhibits a different stress level when it is deformed – even though all the elements are using the same material model (with different material direction vectors). This difference is due to the fact that the material depends on multiple tabulated hardening for each direction and type of deformation. Because these models are single element, the stress vs. strain results for each element match the input yield curve. This modeling technique is very valuable to the material model developer to verify that the model is working appropriately.

4 Full specimen simulations

Physical testing (uniaxial tension and compression) for Al-2024 [7] and Ti-6Al-4V [8] were used to validate the development of this material model. These tests were extracted from a 0.50-inch aluminum rolled plate and a 0.25-inch titanium rolled plate. Each test was designed using a typical uniaxial tension specimen and a cylindrical compression specimen. Since Al-2024 is a face centered

cubic (FCC) material, these materials rarely exhibit significant tension-compression asymmetry [9]. Subsequently, Al-2024 was used to validate the first phase of the model development (tension anisotropy). In contrast, Ti-6Al-4V is a hexagonal closed packed (HCP) metal that exhibits tension-compression asymmetry [9]. Therefore, the titanium specimens are used to validate the second phase of development (tension and compression anisotropy).

Using a single material model, the authors were able to replicate test results for both materials in each specimen direction. The only difference in the material model (from specimen to specimen) was the definition of the material direction relative to the rolling direction.

4.1 Al-2024 tension specimens

In order to accurately simulate the uniaxial tension testing for Al-2024, hardening curves (effective stress as a function of effective plastic strain) for the material were generated. For each test case, the true stress – true strain of the test specimen was calculated and then a set of extrapolated curves were generated after the necking point. Each of these curves were then simulated using the **`*MAT_224`** (isotropic) material model. Once a suitable hardening curve was selected for that specific direction, it was stored for later use. After all the acceptable hardening curves were found (for each direction) then the appropriate curves were used as inputs for the full **`*MAT_264`** anisotropic model. The only difference between each material model was the direction of the material axes (as defined by the **`aopt`** parameter).

Each tension specimen (0-deg, 45-deg, and 90-deg) was then simulated using the full set of hardening curves. These curves included:

- 00-deg tension
- 00-deg compression
- Shear (derived from the 00-deg tension curve)
- 90-deg tension
- 45-deg tension
- Thickness tension (not tested - derived from the ratio of 00-deg tension to 00-deg compression)

The results from these simulations are shown in Figure 3. The test data, in red/green/blue show some mild anisotropy. Even so, the **`*MAT_264`** material model was able to provide very similar results in each of the three directions.

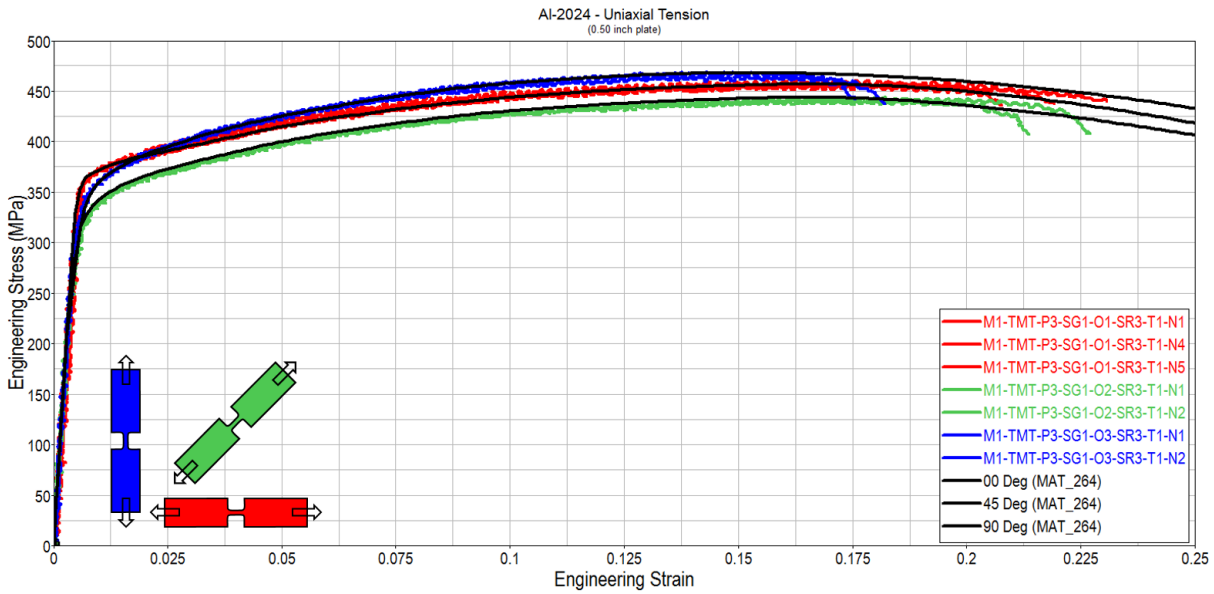

*Fig.3: Engineering stress-strain results from physical tension testing of Al-2024 [7] and simulated results using the *MAT_264 material model*

4.2 Ti-6Al4V tension and compression specimens

The second material used to validate the ***MAT_264** material model is Ti-6Al-4V. This material was tested in both tension and compression for anisotropy. Like the Al-2024 material, input hardening curves were generated from the test data using a similar isotropic model. Once all of the input curves were acceptable, a larger, anisotropic model was compiled. This model included the following curves:

- 00-deg tension
- 00-deg compression
- Shear (derived from the 00-deg tension curve)
- 90-deg tension
- 90-deg compression
- 45-deg tension
- 45-deg compression
- Thickness tension (derived from the ratio of 00-deg tension to 00-deg compression)
- Thickness compression

By using the full ***MAT_264** material model generated from the Ti-6Al-4V test data, each uniaxial tension specimen was simulated. Similar to the aluminum simulations, a single material model was used for all simulations. The results of the physical testing, along with the simulation results, are shown below in Figure 4.

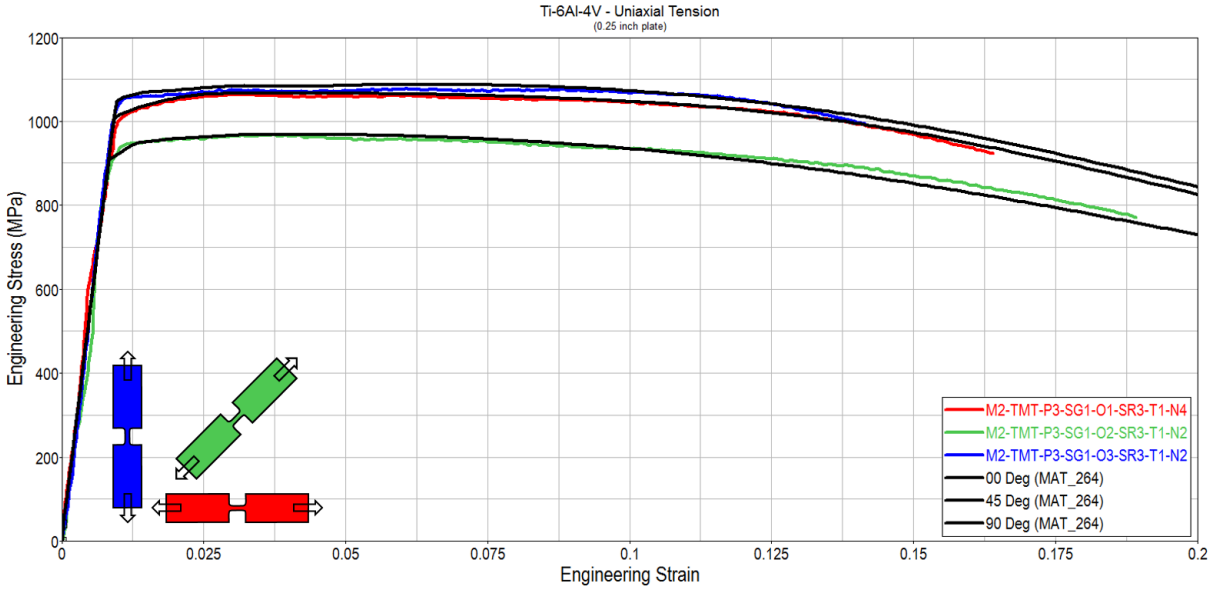

*Fig.4: Engineering stress-strain results from physical tension testing of Ti-6Al-4V [8] and simulated results using the *MAT_264 material model*

In addition to the uniaxial tension testing of Ti-6Al-4V, this material was also tested using four uniaxial compression specimens. Figure 5 shows the engineering stress-strain data provided by the physical testing. As previously assumed, this material exhibits some tension-compression asymmetry. Therefore, this material is an acceptable candidate to validate the second phase of the ***MAT_264** development process.

Similar to the modeling process for uniaxial tension, four hardening curves were generated using the test data from the compression tests individually. Afterwards, these curves were combined into one single material input card. The engineering stress-strain results from the simulations can be seen in Figure 5.

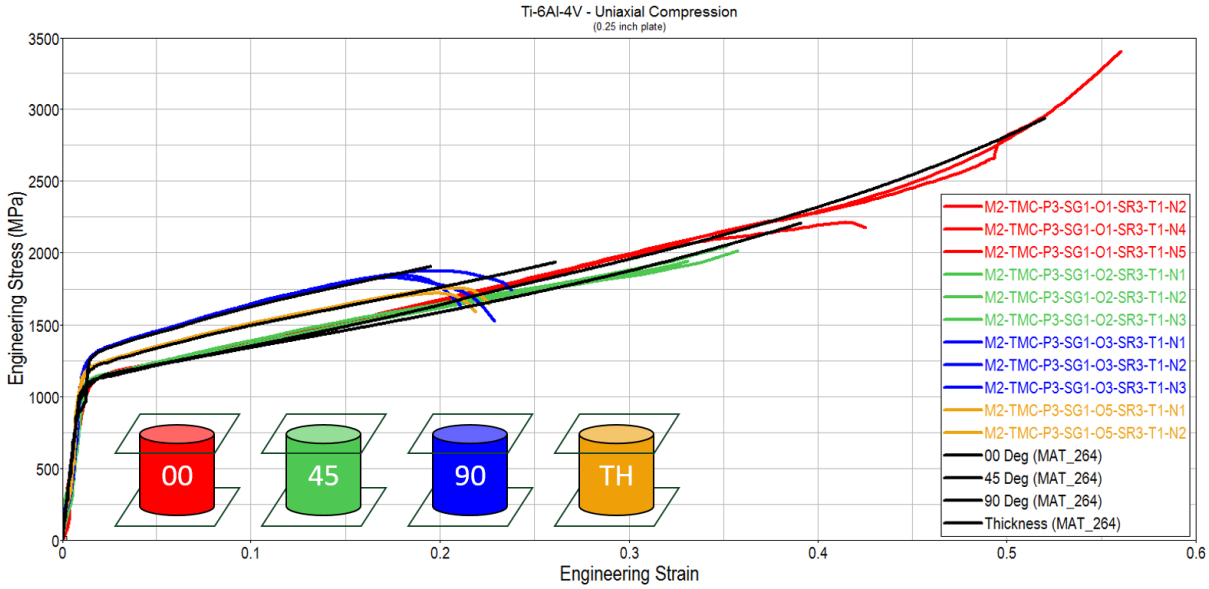

*Fig.5: Engineering stress-strain results from physical compression testing of Ti-6Al-4V [8] and simulated results using the *MAT_264 material model*

5 Summary

This research formally introduces a new material model for simulating crash and impact dynamics for metals using solid elements. In addition to strain rate effects, temperature effects and an isotropic failure model, the effect of material anisotropy is also specified using tabulated hardening curves. Additionally, this model is asymmetric in that it can model elements in tension, compression and shear with tabulated hardening.

The model development is based on a two phase strategy. First, a *Hill* yield function is used instead of a *von-Mises* yield function (used in ***MAT_224_GYS**). Second, two orthotropic Lode parameters are used, in place of a single Lode parameter. This change provided more independent coefficients and a more generalized yield function.

This material model was first verified using single element simulations. First, an isotropic implementation of this model (where all the yield stresses are equal) was verified to replicate similar isotropic material models, such as ***MAT_224_GYS**. Subsequently, an anisotropic implementation of this model (where the yield stresses are not equal) was simulated and compared to the original true stress – true strain input data. These verification models showed consistent and stable results.

The second verification step was to simulate tensile and compressive responses for a single element. By using the anisotropic implementation of ***MAT_264**, elements deformed in tension and compression proved to exhibit a response that matched the tabulated input curves. This was true for all material directions: 00-deg, 45-deg, 90-deg, and thickness directions.

Finally, full size material testing specimens were simulated and compared to physical testing. The test results from two materials (Al-2024 and Ti-6Al-4V) were used to generate two distinct material model input data sets. Each model was subsequently simulated in the 00-deg, 45-deg and 90-directions in uniaxial tension. Additionally, for the titanium material, the compressive response in the 00-deg, 45-deg, 90-deg, and thickness directions were also simulated and compared to the physical testing. These results indicated that ***MAT_264** was able to reproduce remarkably favorable results in both tension and compression for each material direction.

6 Literature

[1] Sengoz, K.: " Development of A Generalized Isotropic Yield Surface for Pressure Insensitive Metal Plasticity Considering Yield Strength Differential Effect in Tension, Compression and Shear Stress States", Doctoral Dissertation (The George Washington University), 2015
[2] Hill, R.: “A theory of the yielding and plastic flow of anisotropic metals”, 1948
[3] Cazacu, O., Barlat, F.: “Application of the theory of representation to describe yielding of anisotropic aluminum alloys”, International Journal of Engineering Science 41, 2003.
[4] Cazacu, O., Barlat, F.: “A criterion for description of anisotropy and yield differential effects in pressure-insensitive metals”, International Journal of Plasticity 20, 2004.
[5] Cazacu, O., Barlat, F.: “Generalization of Drucker’s Yield Criterion to Orthotropy“, Mathematics and Mechanics of Solids 6, 2001.
[6] Barlat, F.: “Linear transfomation-based anisotropic yield functions”, International Journal of Plasticity 21, 2005.
[7] Seidt, J.: “Plastic Deformation and Ductile Fracture of 2024-T351 Aluminum under Various Loading Conditions”, Doctoral Dissertation (The Ohio State University), 2010.
[8] Hammer, J.: “Plastic Deformation and Ductile Fracture of Ti-6Al-4V under Various Loading Conditions”, Thesis (The Ohio State University), 2012.
[9] Lloyd, J., Becker, R.: “A yield surface for HCP materials undergoing a wide range of loading conditions”, The Minerals, Metals, & Materials Society, TMS2015 annual meeting supplemental proceedings, 2015.

7 Acknowledgments

The authors would like to thank the Federal Aviation Administration of the U.S. Department of Transportation for their support of this research.